



**Induction of premature senescence in cardiomyocytes by doxorubicin as a novel mechanism of myocardial damage**

Journal:	<i>Aging Cell</i>
Manuscript ID:	ACE-07-0086.R2
Manuscript Type:	Original Paper
Date Submitted by the Author:	n/a
Complete List of Authors:	Maejima, Yasuhiro; Tokyo Medical and Dental University, Department of Cardiovascular Medicine Adachi, Susumu; Tokyo Medical and Dental University, Department of Cardiovascular Medicine Ito, Hiroshi; Akita University, Department of Cardiovascular Medicine Hirao, Kenzo; Tokyo Medical and Dental University, Department of Cardiovascular Medicine Isobe, Mitsuaki; Tokyo Medical and Dental University, Department of Cardiovascular Medicine; Tokyo Medical and Dental University, Department of Cardiovascular Medicine
Keywords:	cardiac declines with age, p53, cellular senescence, oxidative stress



# Induction of premature senescence in cardiomyocytes by doxorubicin as a novel mechanism of myocardial damage

Yasuhiro Maejima MD, PhD <sup>1)</sup>, Susumu Adachi MD, PhD <sup>1)</sup>,  
Hiroshi Ito MD, PhD <sup>2)</sup>, Kenzo Hirao, MD, PhD <sup>1)</sup>, Mitsuaki Isobe MD, PhD <sup>1)</sup>

1). Department of Cardiovascular Medicine, Tokyo Medical and Dental University

2). Department of Cardiovascular Medicine, Akita University

## Summary

Cellular senescence is an important phenomenon in decreased cellular function. Recently, it was shown that cellular senescence is induced in proliferating cells within a short period of time by oxidative stresses. This phenomenon is known as premature senescence. However, it is still unknown whether premature senescence can be also induced in cardiomyocytes. The aim of the present study was to investigate whether a senescence-like phenotype can be induced in cardiomyocytes by oxidative stress. In cardiomyocytes obtained from aged rats (24 months of age), the staining for senescence-associated  $\beta$ -galactosidase (SA  $\beta$ -gal) increased significantly and the protein or RNA levels of cyclin-dependent kinase inhibitors increased compared to those of young rats. Decreased cardiac troponin I phosphorylation and telomerase activity were also observed in aged cardiomyocytes. Treatment of cultured neonatal rat cardiomyocytes with a low concentration of DOX ( $10^{-7}$  mol/L) did not induce apoptosis but did induce oxidative stress, which was confirmed by 2',7'-dichlorofluorescein diacetate staining. In DOX-treated neonatal cardiomyocytes, increased positive staining for SA  $\beta$ -gal, cdk-I expression, decreased cardiac troponin I phosphorylation, and decreased telomerase activity were observed, as aged cardiomyocytes. Alterations in mRNA expression typically seen in aged cells were observed in DOX-treated neonatal cardiomyocytes. We also found that PML protein and acetylated p53, key proteins involved in stress-induced premature senescence in proliferating cells, were associated with cellular alterations of senescence in DOX-treated cardiomyocytes. In conclusion, cardiomyocytes treated with DOX showed characteristic changes similar to cardiomyocytes of aged rats. PML-related p53 acetylation may be an underlying mechanism of senescence-like alterations in cardiomyocytes. These findings indicate a novel mechanism of myocardial dysfunction induced by oxidative stress.

(*Aging Cell*. 2007 Nov 21 [Epub ahead of print])

\*\*\*\*\*

Correspondence to Susumu Adachi, MD, Department of Cardiovascular Medicine,  
Tokyo Medical and Dental University, 1-5-45 Yushima, Bunkyo, Tokyo 113-8519,  
Japan.

Tel: 81-3-5803-5218, Fax: 81-3-5803-0133

E-mail: [sadachi.cvm@tmd.ac.jp](mailto:sadachi.cvm@tmd.ac.jp)

Key words: premature senescence, oxidative stress, cardiomyocyte, doxorubicin, cell cycle, p53

## Introduction

Cellular senescence is an important factor in decreased cellular function. Hayflick and Moorhead introduced the term cellular senescence to describe the terminal growth arrest that limits continuous propagation of normal human diploid fibroblasts in culture (Hayflick & Moorhead 1961). Recently, it was shown that cellular senescence is induced within a short period of time by exposing cells to subcytotoxic concentrations of oxidants or DNA-damaging agents such as hydrogen peroxide (Chen *et al.* 2000) or to ultraviolet irradiation (Wlaschek *et al.* 2000). This phenomenon is termed stress-induced premature senescence; it occurs when the cell cycle is forcibly and irreversibly arrested (Serrano *et al.* 1997). Proliferating cells in stress-induced premature senescence have features in common with replicative senescence. The senescent phenotypes are associated with a typical gene expression profile (de Magalhaes *et al.* 2004), a senescent morphology, increases in senescence-associated  $\beta$ -galactosidase (SA  $\beta$ -gal) activity (Dimri *et al.* 1995), growth arrest in the G1 phase of the cell cycle (Afshari *et al.* 1993), and shortening of telomere length (Counter 1996). Cardiomyocytes are terminally differentiated cells. Therefore, a different strategy from that for analysis of proliferating cells is necessary to evaluate senescence in these cells. Previous studies have shown that the inotropic response of the heart to  $\beta$ -adrenergic stimulation decreases with age (Li *et al.* 2000). This alteration has been attributed, in part, to an age-related impairment in the phosphorylation of cardiac troponin I (cTnI), which is essential for cardiac muscle contraction (Jiang *et al.* 1993). Several studies have shown that DNA microarrays can be used in cardiovascular aging research to generate panels of hundreds of transcriptional biomarkers (Anisimov *et al.* 2002; Bodyak *et al.* 2002). The gene expression profile of aging cardiomyocyte shows similarities to profiles of known heart disorders, such as ischemic heart disease and cardiomyopathies (Depre *et al.* 1998; Juhasz *et al.* 2002).

In recent years, the roles of cell cycle regulators in cardiomyocytes have been analyzed extensively, revealing that these regulators are closely associated with hypertrophy and apoptosis of cardiomyocytes (Tamamori *et al.* 1998; Adachi *et al.* 2001). Involvement of cell cycle regulatory mechanisms in senescence has been shown in proliferating cells. However, few study of senescence in cardiomyocytes is reported,

because cardiomyocyte is terminally differentiated cell (Torella *et al.* 2004; Park & Prolla 2005). It is important to determine whether cell cycle regulators play key roles in senescence of cardiomyocytes.

Oxidative stress is responsible for the pathogenesis of various diseases and has been shown to play a role in the aging process. Doxorubicin (DOX) is an antitumor anthracycline antibiotic and is found to increase oxidative stress. Low concentrations of DOX can induce terminal growth arrest with senescence-like alterations in proliferating cells (Rebbaa *et al.* 2003). The aim of the present study was to investigate whether a senescence-like phenotype can be induced in cardiomyocytes by oxidative stress with low concentrations of DOX and to compare any changes with age-related changes. We also studied the underlying mechanisms of premature senescence in cardiomyocytes.

## Results

### DOX induced oxidative stress but did not induce apoptosis in cardiomyocytes

DOX was known to increase the cytosolic formation of superoxide anions and to decrease cardiomyocyte viability (Zhou *et al.* 2001). We examined the concentration-dependent effect of DOX on cardiomyocyte apoptosis. Treatment of cultured cells with  $10^{-6}$  mol/L DOX elicited caspase-3 cleavage and DNA fragmentation. However, treatment with  $10^{-7}$  mol/L DOX had minimal effects (Figure 1A-C). To determine whether treatment with DOX induced oxidative stress, we used the oxidant-sensitive fluorescent probe, 2',7'-dichlorofluorescein diacetate (DCFH-DA). Cardiomyocytes treated with  $H_2O_2$  ( $10^{-5}$  mol/L) were used as a positive control for oxidative stress. Treatment of cardiomyocytes with DOX ( $10^{-6}$  mol/L or  $10^{-7}$  mol/L) or  $H_2O_2$  ( $10^{-5}$  mol/L) showed increased fluorescence intensity, indicating an increase in dichlorofluorescein (DCF) production (Figure 1D). Thus,  $10^{-7}$  mol/L DOX induced oxidative stress but did not induce apoptosis in cardiomyocytes.

### Aged and DOX-treated cardiomyocytes showed increased numbers of SA $\beta$ -gal-positive cells

Cardiomyocytes are terminally differentiated; therefore, DOX treatment does not induce growth arrest in these cells. However, cardiomyocytes may show a physiologic effect of DOX-induced

oxidative stress. Quantification of SA  $\beta$ -gal activity is useful to evaluate cell senescence activity (Dimri *et al.* 1995). To investigate whether cardiomyocytes treated with a low concentration of DOX showed a senescent phenotype, we examined SA  $\beta$ -gal activity in cultured neonatal rat cardiomyocytes incubated with  $10^{-7}$  mol/L DOX for 7 days. The percentage of SA  $\beta$ -gal-positive cells increased significantly compared to that among control cells (control:  $0.33 \pm 0.15\%$ , DOX-treated:  $2.43 \pm 0.8\%$ ,  $H_2O_2$ -treated:  $1.85 \pm 0.9\%$ ,  $n=3$ ,  $P<0.05$ ; Figure 2A-B). We also assessed SA  $\beta$ -gal staining at different ages (Figure 2C). The percentage of SA  $\beta$ -gal-positive cells was determined by counting positive cells in a cross-section of the heart. SA  $\beta$ -gal-positive cells in young (2-month-old) rats comprised  $0.13 \pm 0.05\%$ , in 11-month-old rats comprised  $0.4 \pm 0.1\%$ , and in aged (24-month-old) rats comprised  $0.9 \pm 0.2\%$  ( $n=3$ ,  $P<0.05$ ; Figure 2D). In DOX-induced cardiomyopathy model rats, the ratio of SA  $\beta$ -gal-positive cardiomyocytes was significantly increased than that of age-matched (11-month-old) control rats ( $1.9 \pm 0.9\%$ ,  $n=3$ ,  $P<0.05$ ; Figure 2C-D). These results indicate that the number of SA  $\beta$ -gal-positive cells increased among aged and in DOX-treated cardiomyocytes.

#### **Troponin I phosphorylation was decreased in aged and DOX-treated cardiomyocytes**

To examine the effect of age and DOX treatment on phosphorylation of cTnI, we performed immunoblot analysis with a phospho-specific antibody that recognizes cTnI phosphorylation. As reported previously, cardiomyocytes from aged rats showed less phosphorylation of cTnI than did those from young rats (Figure 3A) (Sakai *et al.* 1989; Jiang *et al.* 1993). Cultured neonatal cardiomyocytes pretreated with DOX significantly decreased cTnI phosphorylation, relative to untreated cardiomyocytes (Figure 3B). Thus, the baseline of cTnI phosphorylation level was decreased in aged as well as in DOX-treated cardiomyocytes.

Next, to estimate the change of the decreased cTnI phosphorylation seen in DOX-treated neonatal cardiomyocytes, we examined the troponin I phosphorylation response to  $\beta$ -adrenoceptor stimulation by isoproterenol (ISP,  $10^{-6}$  mol/L). As shown in Figure 3C, in untreated cardiomyocytes, ISP induced a large and significant increase in cTnI phosphorylation. The cardiomyocytes, treated with DOX revealed significantly delayed response in cTnI

phosphorylation. These data indicate that treatment of DOX attenuates ISP-induced cTnI phosphorylation in cardiomyocytes.

#### **Altered gene expression in aged and DOX-treated cardiomyocytes**

To evaluate changes of expression of cardiac-specific genes, mRNA levels of several genes were analyzed in cardiomyocytes from young and aged rats by Northern blotting. As shown in previous gene expression arrays studies (Anisimov *et al.* 2002; Bodyak *et al.* 2002), mRNA levels of SERCA2,  $\alpha$ -MHC, GATA4 and Nkx2.5 were downregulated and those of ANP and angiotensin II receptor were upregulated with age. We then evaluated these mRNA levels in neonatal cardiomyocytes in response to a low concentration of DOX. mRNA levels of SERCA2,  $\alpha$ -MHC, GATA4 and Nkx2.5 were downregulated, and those of ANP and angiotensin II receptor were upregulated in a time-dependent manner (Figure 4). These results indicate that DOX can induce some of the transcriptional alterations that occur with age.

#### **Attenuation of telomerase activity in aged and DOX-treated cardiomyocytes**

To determine whether young and aged rat hearts differ with respect to telomerase activity and to compare the telomerase activity in control vs. DOX-treated cardiomyocytes, we assayed telomerase activity by the telomeric repeat amplification protocol (TRAP) assay. In DOX-treated neonatal cardiomyocytes, telomerase activity was decreased in a time-dependent manner (Figure 5A). Consistent with the loss of telomerase activity and decreased telomere length, the level of telomerase reverse transcriptase (TERT) protein detected by immunoblotting was prominent in neonatal and young rat myocardium and was down-regulated in aged heart. In DOX-treated neonatal cardiomyocytes, TERT protein level was also decreased in a time-dependent manner (Figure 5B). Furthermore, to assess whether young and aged rat hearts or untreated and DOX treated cardiomyocytes differ with respect to telomere length, quantitative fluorescence *in situ* hybridization (Q-FISH) was performed using a telomere-specific peptide nucleic acid (PNA) probe. Fluorescence intensity was significantly weaker in aged rat cardiomyocytes compared with young rat cardiomyocytes (Fig. 5C (1) - (2)). Also, we compared the telomere length in untreated and

DOX treated cardiomyocytes, DOX-treated cultured cardiomyocytes had also reduced mean fluorescence intensity compared with that of the untreated cells (Fig. 5C (3) - (4)). Thus, telomere length is shortened in aged as well as in DOX-treated cardiomyocytes.

#### Altered cell cycle regulatory protein expression in aged and DOX-treated cardiomyocytes

To determine whether the protein levels of cdk-Is change with age, we used immunoblotting to examine several cdk-Is. The protein levels of p27<sup>kip1</sup> and p21<sup>cip1/waf1</sup> increased in aged vs. young rat cardiomyocytes (Figure 6A). In cultured neonatal rat cardiomyocytes treated with 10<sup>-7</sup> mol/L DOX, the levels of p27<sup>kip1</sup> and p21<sup>cip1/waf1</sup> were increased in a time-dependent manner. The mRNA level of p16<sup>INK4a</sup> was also upregulated in both aged and DOX-treated cardiomyocytes by reverse-transcription polymerase chain reaction (RT-PCR) analysis (Figure 6B). To elucidate the mechanism underlying the upregulation of p21<sup>cip1/waf1</sup> in aged and DOX-treated cardiomyocytes, we examined the expression of promyelocytic leukemia protein (PML), a key factor in stress-induced premature senescence in proliferating cells (Ferbeyre *et al.* 2000). PML forms a complex with acetylated p53 to activate p21<sup>cip1/waf1</sup> and then induces cell-cycle arrest (Pearson *et al.* 2000; Bischof *et al.* 2002). Immunoblot analysis showed that the PML protein level in aged cardiomyocytes was greater than that in young cardiomyocytes (Figure 6C). However, the shc<sup>P66</sup> adaptor protein, another key factor in stress-induced premature senescence in proliferating cells, was not increased in aged or in DOX-treated cells (Figure 6C). The acetylated form of p53 was increased in aged cardiomyocytes. DOX-treated cardiomyocytes also showed increased PML protein and acetylated p53 in a time-dependent manner. Furthermore, immunoprecipitation and immunoblotting with PML antibody showed that PML formed a complex with p53 and that acetylated p53 was increased in response to DOX treatment (Figure 6D).

To verify the role of the PML-acetylated p53 complex in DOX-treated cardiomyocytes, we used pifithrin- $\alpha$ , an inhibitor of p53 expression (Liu *et al.* 2004), and resveratrol, an inhibitor of p53 acetylation (Howitz *et al.* 2003). In cardiomyocytes treated with DOX and pifithrin- $\alpha$ , the protein levels of both p53 and p21<sup>cip1/waf1</sup> were decreased (Figure 7A). In cardiomyocytes treated with DOX and resveratrol,

the degree of p53 acetylation and the protein level of p21<sup>cip1/waf1</sup> were decreased. In addition, the numbers of SA- $\beta$ -gal-positive cells treated with DOX and pifithrin- $\alpha$  or resveratrol were decreased compared to that in DOX-treated cells (Figure 7B). And, cTnI phosphorylation response to  $\beta$ -adrenoceptor stimulation and telomerase activity in cardiomyocytes treated with DOX and pifithrin- $\alpha$  or resveratrol were enhanced compared to that in DOX-treated cells (Figure 7C-D). These results provide support for the hypothesis that cell cycle regulatory proteins are involved in inducing a senescence-like phenotype in cardiomyocytes.

#### Discussion

The result of this study show that a low concentration of DOX-induced characteristic changes in cardiomyocytes that were similar to those in aged cardiomyocytes and that PML-related p53 acetylation may be the underlying mechanism of senescence-like alterations in cardiomyocytes. Cellular senescence in proliferating cells is a permanent arrest of the cell-cycle that can be triggered by a variety of stressors, including short telomeres and activated oncogenes, and is characterized by a modest increase in the number of SA  $\beta$ -gal-positive cells and by changes in the expression of cdk-Is. Senescence can be induced by oncogenes and DNA damaging agents including DOX, suggesting that it is a tumor-suppressor mechanism, blocking the proliferation of cells with the potential of becoming malignantly-transformed. Contrary to its effects in proliferating cells, cellular senescence in differentiated cardiomyocytes has been difficult to evaluate. In this study, we analyzed characteristics of senescence in cardiomyocytes. Decreased troponin I phosphorylation and changes in the expression of various genes have been reported in cardiomyocytes from aged rat heart (Jiang *et al.* 1993; Bodyak *et al.* 2002). We evaluated changes in the expression of several aging-related genes to confirm senescence in cardiomyocytes, and showed that the age-related expression of several genes in cultured neonatal cardiomyocytes was similar to that in response to DOX. Telomerase replaces telomeric repeat DNA lost during the cell-cycle, restoring telomere length. This enzyme is thought to be expressed only during periods of cell replication, and its activity reflects the extent of proliferation. However, some recent studies have shown that telomerase activity is detectable in

cardiomyocytes and may play an important role in protecting against cell death. Leri reported that aging decreases telomerase activity by 31% in male rat heart cells (Leri *et al.* 2000). Oh reported that telomerase activity and TERT expression are both markedly downregulated in the adult rat heart (Oh & Schneider 2002). Therefore, we investigated changes in telomerase activity as a marker of senescence. Telomerase activity decreased in DOX-treated cardiomyocytes, similar to the decrease induced by age, suggesting that premature senescence is inducible in response to oxidative stress in cardiomyocytes. Premature senescence in vascular endothelial cells is known to be involved in the progression of arteriosclerosis. Minamino reported that vascular endothelial cells with a senescence-associated phenotype are present in atherosclerotic lesions in humans, and endothelial cell senescence induced by telomere shortening may contribute to atherogenesis (Minamino *et al.* 2002). Our results also suggest that senescence of cardiomyocytes in response to oxidative stress may contribute to heart dysfunction.

There are several reports that premature senescence is associated with the irreversible arrest of the cell-cycle mediated by activation of inhibitory cell cycle regulators. Delayed stress-induced premature senescence occurs in light-skinned populations due to a decreased association of p16<sup>INK4a</sup> with cdk4 and decreased phosphorylation of the Rb protein in melanocytes (Toussaint *et al.* 2000). Ras activation through phosphorylation of shc<sup>P66</sup> (Ravichandran 2001; Trinei *et al.* 2002), activation of the MKK7-JNK pathway (MacLaren *et al.* 2004; Wada *et al.* 2004) and p21<sup>cip1/waf1</sup> activation by complex formation of PML with acetylated p53 induce senescence in proliferating cells (Pearson *et al.* 2000; Salomoni & Pandolfi 2002). Oncogenic Ras induces upregulation of PML expression, acetylation of p53, relocalization of p53 and CREB binding protein (CBP) acetyltransferase within PML nuclear bodies, and the formation of a trimeric p53-PML-CBP complex, which in turn facilitates transcriptional activation, resulting in the upregulation of p21<sup>cip1/waf1</sup> and subsequent growth arrest. We previously reported that cardiomyocyte hypertrophy is inhibited when inhibitory components of cell cycle regulators are activated (Tamamori *et al.* 1998). In the present study, we found that PML protein levels were increased and p53 acetylation was facilitated in cardiomyocytes with age or DOX stimulation. DOX-induced senescent alterations were suppressed by the inhibition of p53 expression or

p53 acetylation. Thus, p21<sup>cip1/waf1</sup> activation by the PML-acetylated p53 complex may provide information regarding the mechanisms of premature senescence in cardiomyocytes.

Recent investigations have suggested that cardiac stem cells play important roles in the maintenance of cardiac function and that the loss of functionally competent cardiac stem cells by premature senescence in chronic cardiomyopathy may underlie progressive functional deterioration and the onset of terminal failure (Nadal-Ginard *et al.* 2003; Torella *et al.* 2004; Urbanek *et al.* 2005). However, premature senescence in differentiated cardiomyocytes has not been well characterized. The present study is the first to show that premature senescence can be induced in cardiomyocytes by a low concentration of DOX. p21<sup>cip1/waf1</sup> activation by the PML-acetylated p53 complex may play an important role in this premature senescence. Premature senescence of cardiomyocytes may be a previously unknown mechanism of heart failure. Additional studies will clarify the role of premature senescence in the pathogenesis of heart failure and may lead to the development of novel therapeutic strategies for heart failure.

## Experimental procedures

### Reagents

The following materials were obtained: Eagle's Minimum Essential Medium (MEM), Dulbecco's Modified Eagle Medium (DMEM), calf serum (CS), 5-bromo-4-chloro-3-indolyl  $\beta$ -D galactoside (X-gal) and DOX (doxorubicin hydrochloride) were from Sigma-Aldrich; pifithrin- $\alpha$  and resveratrol were from Calbiochem; antibodies to p16<sup>INK4a</sup>, p21<sup>cip1/waf1</sup>, p27<sup>kip1</sup>, TERT and PML were from Santa Cruz Biotechnologies; antibodies to cTnI and phospho-cTnI were from Cell Signaling Technologies; antibody to p53 was from Oncogene Research Products; antibody to acetyl-p53 (Lys373&382) was from Upstate; antibody to shc was from BD Biosciences; antibody to phospho-shc<sup>P66</sup> (Ser36) was from nanoTools Antikoerpertechnik; secondary antibodies conjugated to horseradish peroxidase and enhanced chemiluminescence reagents were from Amersham and Immobilon-P transfer membrane for immunoblot was from Millipore.

### Animals

Male Wistar rats (4 weeks old; 200-250 g) were purchased from Sankyo Laboratories. Rats were

provided with a standard diet and water and were maintained for 24 weeks in compliance with the Animal Welfare Guidelines of the Institute of Experimental Animals of Tokyo Medical and Dental University.

### Cell culture and treatment

Neonatal cardiomyocytes from 1- or 2-day-old rats were isolated, subjected to Percoll gradient centrifugation and cultured in vitro as described previously (Maejima *et al.* 2003). Cardiomyocytes were incubated in MEM supplemented with 5% CS for 24 hours at 37°C and then subjected to treatment with  $10^{-7}$  mol/L-DOX in MEM plus 5% CS at 37°C for various periods. All experiments were performed in accordance with the Guide for the Care and Use of Laboratory Animals (NIH Publication No. 85-23, revised 1996) and were approved by the Animal Research Committee of the Tokyo Medical and Dental University.

### DOX-induced cardiomyopathy model

DOX-induced cardiomyopathy was generated as previously described (Siveski-Iliskovic *et al.* 1995). Male Wistar rats (6-weeks old) weighing 180 to 220 g were used. DOX was administered intraperitoneally in 6 equal injections (each containing 2.5 mg/kg) over a period of two weeks, with a total cumulative dosage of 15mg/kg body weight. These rats were sacrificed at 11-month old.

### Analysis of DNA fragmentation

DNA released from cells was extracted and separated by electrophoresis on 2% agarose gels containing 0.1  $\mu$ g ethidium bromide and visualized under UV light as described previously (Adachi *et al.* 2001).

### Visualization of alterations due to oxidative stress

The compound DCFH-DA is a useful fluorescent marker of oxidative stress (Sarvazyan 1996). The esterified form of DCFH-DA rapidly penetrates cell membranes and is deacetylated by intracellular esterases. Nonfluorescent DCFH is then trapped in the cytosol and, upon oxidation to DCF, serves as a sensitive cytosolic marker of oxidative stress. Cardiomyocytes were preincubated with  $10^{-5}$  mol/L DCFH for 40 minutes in MEM containing  $1.25 \times 10^{-3}$  mol/L

$\text{CaCl}_2$ , 1% bovine serum albumin, and  $25 \times 10^{-3}$  mol/L

N-2-hydroxyethylpiperazine-N'-2-ethanesulfonic acid (pH 7.3). Cells were observed with a phase-contrast microscope (Olympus). Excitation of DCF was achieved with the 488-nm line of a 15-mW argon-ion laser attenuated to 1% intensity. Emitted light was collected through an emission filter of 505 nm.

### SA $\beta$ -Gal staining

SA  $\beta$ -gal staining was performed as described previously (Dimri *et al.* 1995). In brief, cryostat sections were fixed in 3% formaldehyde for 15 minutes, followed by 3 washes in phosphate buffered saline (PBS) at room temperature. Slides were immersed in freshly prepared SA  $\beta$ -gal staining solution [1 mg/mL X-gal in dimethylformamide,  $40 \times 10^{-3}$  mol/L citric acid, sodium phosphate (pH 6.0),  $5 \times 10^{-3}$  mol/L potassium ferrocyanide,  $5 \times 10^{-3}$  mol/L potassium ferricyanide,  $150 \times 10^{-3}$  mol/L NaCl and  $2 \times 10^{-3}$  mol/L  $\text{MgCl}_2$ ] and incubated at 37°C for overnight. Stained sections were washed twice with PBS and counterstained for 1 minute with hematoxylin. Excess counterstain was removed with 2 washes in PBS. Cultured cardiomyocytes were also subjected to SA  $\beta$ -gal staining, and cardiomyocytes were identified with a  $\alpha$ -sarcomeric actin antibody and 3-amino-9-ethylcarbazole as a chromogen. Samples were analyzed by 2 independent investigators in a blind fashion. All samples were stained in triplicate.

### Immunoblotting

Electrophoresis was performed on 10% sodium dodecyl sulfate-polyacrylamide gels. Gels were transferred to PVDF membranes by semi-dry electrotransfer, and immunoblotting was performed as described previously (Maejima *et al.* 2003). All experiments were evaluated by densitometric analysis with Image J software (National Institutes of Health, Bethesda, MD).

### RT-PCR

Total RNA from neonatal rat cardiomyocytes was isolated by the guanidium thiocyanate-phenol -chloroform method with ISOGEN reagent (Nippon Gene). cDNA was prepared from 5  $\mu$ g of RNA by reverse transcription. cDNA (10  $\mu$ L) was amplified. Polymerase chain reaction products were analyzed by ethidium bromide staining of

1.5% agarose gels.

### Northern blot analysis

Northern blot analysis was performed as described previously (Tamamori *et al.* 1998). In brief, RNA (10  $\mu$ g) was size fractionated through a 1.4% agarose gel in 0.7 mol/L formaldehyde and  $20 \times 10^{-3}$  mol/L morpholinopropanesulfonic acid,  $5 \times 10^{-3}$  mol/L sodium acetate, and  $1 \times 10^{-3}$  mol/L ethylenediaminetetraacetic acid (EDTA). Hybridization was performed in hybridization buffer containing 50% formamide,  $5 \times$  Denhardt's solution, 100 mg/mL salmon sperm DNA, and  $5 \times$  SSPE (0.75 mol/L NaCl, 0.05 mol/L  $\text{NaH}_2\text{PO}_4$ ,  $5 \times 10^{-3}$  mol/L EDTA).  $^{32}\text{P}$ -labeled cDNA probes were prepared by the random primer method. Membranes (Managrap nylon; Micron Separations) were washed twice with  $5 \times$  SSPE/10% SDS at room temperature, once with  $2 \times$  SSPE/10% SDS at  $37^\circ\text{C}$ , and once with  $0.2 \times$  SSPE/10% SDS at  $37^\circ\text{C}$  for 15 minutes each. Autoradiography was performed on MP film (Amersham) with an intensifying screen at  $-80^\circ\text{C}$ . Radioactivities were quantified with a BAS 2500 densitometer (Fuji Film Corp.). Results were normalized to GAPDH expression.

### Telomeric repeat amplification

TRAP assay was performed using a TRAPeze® telomerase Detection Kit (Intergen, Purchase, NY) according to the manufacturer's protocol with some modifications (Bae *et al.* 2007). Cardiomyocytes were lysed in 3-[(3-cholamidopropyl) dimethyl-ammonio]-1-propanesulfonate buffer, incubated on ice for 30 minutes, and centrifuged at  $14,000 \times g$  for 20 min at  $4^\circ\text{C}$ . For neonatal rats, 2  $\mu$ g of cardiomyocyte extract was used. In adult rats, 2  $\mu$ g of untreated myocyte extract and extract treated with RNase were incubated with telomerase substrate (TS oligonucleotide: 5'-AAT CCG TCG AGC AGA GTT-3') for 30 minutes in the following solution:  $20 \times 10^{-3}$  mol/L Tris-HCl, pH 8.3,  $1.5 \times 10^{-3}$  mol/L  $\text{MgCl}_2$ ,  $68 \times 10^{-3}$  mol/L KCl,  $1 \times 10^{-3}$  mol/L O,O'-Bis(2-aminoethyl)ethyleneglycol -N,N,N',N'-tetraacetic acid, 0.05% Tween 20,  $50 \times 10^{-3}$  mol/L deoxynucleotide triphosphates, 2 units Taq DNA polymerase and 0.1  $\mu$ g anchored reverse primer (5'-GCG CGC [CTTACC]<sub>3</sub> CTA ACC-3'). Samples were subjected to 31 amplification cycles of  $94^\circ\text{C}$  for 30 seconds,  $50^\circ\text{C}$  for 30 seconds and  $72^\circ\text{C}$  for 3 minutes. PCR products were separated on 12% polyacrylamide

gels and visualized with SYBR® Green I Nucleic Acid Gel Stain (Molecular Probes, Inc. Eugene, OR) as described in the manufacturer's protocol. The stained bands were visualized and photographed using a UV light source (300 nm transilluminator). We used the internal standards to compare the relative telomerase activity. Additionally, HeLa cell extracts (1  $\mu$ g) were also used as a positive control. Densitometric analysis was done with Image J software.

### Q-FISH

Telomere length in cardiomyocyte nuclei was evaluated in tissue sections or cultured cardiomyocytes grown on glass coverslips by measuring the Q-FISH (Wiemann *et al.* 2002; Nakajima *et al.* 2004). After fixation by 4% paraformaldehyde for 5 min, each slide was dehydrated using an increasing ethanol series (70%, 85% and 95%, at  $-20^\circ\text{C}$ ) and air-dried. Then, each slides were autoclaved at  $95^\circ\text{C}$  for 40 min in Target Retrieval Solution (No. S1700, DAKO, Denmark). After cooling to room temperature for 20 min, the slides were washed in deionized water for 1 min three times, and immersed in 0.3%  $\text{H}_2\text{O}_2$ /absolute methanol at room temperature for 20 min to block endogenous peroxidase. The slides were pre-treated with proteinase K for 10 min and washed twice. Fluorescent isothiocyanate-labelled PNA telomere-specific probe (10  $\mu$ L) was applied to each specimen (K5325 (Telomere PNA FISH kit); Dako, Denmark), which was covered with a coverslip. The probe was denatured on a heat block at  $90^\circ\text{C}$  for 5 min, and slides were then moved to a dark moisture chamber at  $45^\circ\text{C}$  overnight. Coverslips were carefully removed in Tris-buffered saline containing Tween 20 (TBST; 50mM Tris-HCL, 0.3 M NaCl, 0.1% Tween 20, pH 7.8) and the slides were washed in wash solution at a dilution of 1:50 at  $52^\circ\text{C}$  for 20 min. The slides were rehydrated by decreasing the ethanol series, immersed in TBST, counterstained with 4'-6-diamidino-2-phenylindole (DAPI; 1  $\mu$ g/mL), and finally mounted with PermaFluor® (Thermo Shandon, Pittsburgh, PA). Fluorescent telomere labelling from single nuclei was observed by laser scanning confocal microscope (LSM510, Carl Zeiss, Jena, Germany). Fluorescence was quantified using Image J software. No fluorescent telomere labelling was observed when no probe was present at the hybridization stage of the Q-FISH protocol.



## Statistical analysis

Data are shown as mean  $\pm$  standard deviation values. Differences were analyzed with one-way analysis of variance (ANOVA), and post-hoc analysis was performed with a Bonferroni/Dunn test.  $P < 0.05$  was considered significant.

## Acknowledgements

This study was supported by a Grant-in-Aid for Scientific Research from the Ministry of Education, Science and Culture of Japan, a Research Grant for Diseases from the Ministry of Health and Welfare of Japan, and a Grant from the Japan Cardiovascular Research Foundation.

## References

- Adachi S, Ito H, Tamamori-Adachi M, Ono Y, Nozato T, Abe S, Ikeda M, Marumo F, Hiroe M (2001). Cyclin A/cdk2 activation is involved in hypoxia-induced apoptosis in cardiomyocytes. *Circ Res.* 88, 408-414.
- Afshari CA, Vojta PJ, Annab LA, Futreal PA, Willard TB, Barrett JC (1993). Investigation of the role of G1/S cell cycle mediators in cellular senescence. *Exp Cell Res.* 209, 231-237.
- Anisimov SV, Tarasov KV, Stern MD, Lakatta EG, Boheler KR (2002). A quantitative and validated SAGE transcriptome reference for adult mouse heart. *Genomics.* 80, 213-222.
- Bae SN, Kim J, Lee YS, Kim JD, Kim MY, Park L-O (2007). Cytotoxic effect of zinc-citrate compound on choriocarcinoma cell lines. *Placenta.* 28, 22-30.
- Bischof O, Kirsh O, Pearson M, Itahana K, Pelicci PG, Dejean A (2002). Deconstructing PML-induced premature senescence. *EMBO J.* 21, 3358-3369.
- Bodyak N, Kang PM, Hiromura M, Suljoadikusumo I, Horikoshi N, Khrapko K, Usheva A (2002). Gene expression profiling of the aging mouse cardiac myocytes. *Nucleic Acids Res.* 30, 3788-3794.
- Chen QM, Tu VC, Liu J (2000). Measurements of hydrogen peroxide induced premature senescence: senescence-associated beta-galactosidase and DNA synthesis index in human diploid fibroblasts with down-regulated p53 or Rb. *Biogerontology.* 1, 335-339.
- Counter CM (1996). The roles of telomeres and telomerase in cell life span. *Mutat Res.* 366, 45-63.
- de Magalhaes JP, Chainiaux F, de Longueville F, Mainfroid V, Migeot V, Marcq L, Remacle J, Salmon M, Toussaint O (2004). Gene expression and regulation in H<sub>2</sub>O<sub>2</sub>-induced premature senescence of human foreskin fibroblasts expressing or not telomerase. *Exp Gerontol.* 39, 1379-1389.
- Depre C, Shipley GL, Chen W, Han Q, Doenst T, Moore ML, Stepkowski S, Davies PJ, Taegtmeier H (1998). Unloaded heart in vivo replicates fetal gene expression of cardiac hypertrophy. *Nat Med.* 4, 1269-1275.
- Dimri GP, Lee X, Basile G, Acosta M, Scott G, Roskelley C, Medrano EE, Linskens M, Rubelj I, Pereira-Smith O, et al. (1995). A biomarker that identifies senescent human cells in culture and in aging skin in vivo. *Proc Natl Acad Sci U S A.* 92, 9363-9367.
- Ferbeyre G, de Stanchina E, Querido E, Baptiste N, Prives C, Lowe SW (2000). PML is induced by oncogenic ras and promotes premature senescence. *Genes Dev.* 14, 2015-2027.
- Hayflick L, Moorhead PS (1961). The serial cultivation of human diploid cell strains. *Exp Cell Res.* 25, 585-621.
- Howitz KT, Bitterman KJ, Cohen HY, Lamming DW, Lavu S, Wood JG, Zipkin RE, Chung P, Kisielewski A, Zhang LL, Scherer B, Sinclair DA (2003). Small molecule activators of sirtuins extend *Saccharomyces cerevisiae* lifespan. *Nature.* 425, 191-196.
- Jiang MT, Moffat MP, Narayanan N (1993). Age-related alterations in the phosphorylation of sarcoplasmic reticulum and myofibrillar proteins and diminished contractile response to isoproterenol in intact rat ventricle. *Circ Res.* 72, 102-111.
- Juhasz O, Zhu Y, Garg R, Anisimov SV, Boheler KR (2002). Analysis of altered genomic expression profiles in the senescent and diseased myocardium using cDNA microarrays. *Eur J Heart Fail.* 4, 687-697.
- Leri A, Malhotra A, Liew CC, Kajstura J, Anversa P (2000). Telomerase activity in rat cardiac myocytes is age and gender dependent. *J Mol Cell Cardiol.* 32, 385-390.
- Li L, Desantiago J, Chu G, Kranias EG, Bers DM (2000). Phosphorylation of phospholamban and troponin I in beta-adrenergic-induced acceleration of cardiac relaxation. *Am J Physiol Heart Circ Physiol.* 278, H769-779.
- Liu X, Chua CC, Gao J, Chen Z, Landy CL, Hamdy R, Chua BH (2004). Pifithrin-alpha protects against doxorubicin-induced apoptosis and acute cardiotoxicity in mice. *Am J Physiol Heart Circ Physiol.* 286, H933-939.
- MacLaren A, Black EJ, Clark W, Gillespie DA (2004). c-Jun-deficient cells undergo premature

- senescence as a result of spontaneous DNA damage accumulation. *Mol Cell Biol.* 24, 9006-9018.
- Maejima Y, Adachi S, Ito H, Nobori K, Tamamori-Adachi M, Isobe M (2003). Nitric oxide inhibits ischemia/reperfusion-induced myocardial apoptosis by modulating cyclin A-associated kinase activity. *Cardiovasc Res.* 59, 308-320.
- Minamino T, Miyauchi H, Yoshida T, Ishida Y, Yoshida H, Komuro I (2002). Endothelial cell senescence in human atherosclerosis: role of telomere in endothelial dysfunction. *Circulation.* 105, 1541-1544.
- Nadal-Ginard B, Kajstura J, Leri A, Anversa P (2003). Myocyte death, growth, and regeneration in cardiac hypertrophy and failure. *Circ Res.* 92, 139-150.
- Nakajima T, Katagishi T, Moriguchi M, Sekoguchi S, Nishikawa T, Takashima H, Watanabe T, Kimura H, Minami M, Itoh Y, Kagawa K, Okanoue T (2004). Tumor size-independence of telomere length indicates an aggressive feature of HCC. *Biochem Biophys Res Commun.* 325, 1131-1135.
- Oh H, Schneider MD (2002). The emerging role of telomerase in cardiac muscle cell growth and survival. *J Mol Cell Cardiol.* 34, 717-724.
- Park SK, Prolla TA (2005). Gene expression profiling studies of aging in cardiac and skeletal muscles. *Cardiovasc Res.* 66, 205-212.
- Pearson M, Carbone R, Sebastiani C, Cioce M, Fagioli M, Saito S, Higashimoto Y, Appella E, Minucci S, Pandolfi PP, Pelicci PG (2000). PML regulates p53 acetylation and premature senescence induced by oncogenic Ras. *Nature.* 406, 207-210.
- Ravichandran KS (2001). Signaling via Shc family adapter proteins. *Oncogene.* 20, 6322-6330.
- Rebbaa A, Zheng X, Chou PM, Mirkin BL (2003). Caspase inhibition switches doxorubicin-induced apoptosis to senescence. *Oncogene.* 22, 2805-2811.
- Sakai M, Danziger RS, Staddon JM, Lakatta EG, Hansford RG (1989). Decrease with senescence in the norepinephrine-induced phosphorylation of myofilament proteins in isolated rat cardiac myocytes. *J Mol Cell Cardiol.* 21, 1327-1336.
- Salomoni P, Pandolfi PP (2002). The role of PML in tumor suppression. *Cell.* 108, 165-170.
- Sarvazy N (1996). Visualization of doxorubicin-induced oxidative stress in isolated cardiac myocytes. *Am J Physiol.* 271, H2079-2085.
- Serrano M, Lin AW, McCurrach ME, Beach D, Lowe SW (1997). Oncogenic ras provokes premature cell senescence associated with accumulation of p53 and p16INK4a. *Cell.* 88, 593-602.
- Siveski-Iliskovic N, Hill M, Chow DA, Singal PK (1995). Probucol protects against adriamycin cardiomyopathy without interfering with its antitumor effect. *Circulation.* 91, 10-15.
- Tamamori M, Ito H, Hiroe M, Terada Y, Marumo F, Ikeda MA (1998). Essential roles for G1 cyclin-dependent kinase activity in development of cardiomyocyte hypertrophy. *Am J Physiol.* 275, H2036-2040.
- Torella D, Rota M, Nurzynska D, Musso E, Monsen A, Shiraishi I, Zias E, Walsh K, Rosenzweig A, Sussman MA, Urbanek K, Nadal-Ginard B, Kajstura J, Anversa P, Leri A (2004). Cardiac stem cell and myocyte aging, heart failure, and insulin-like growth factor-1 overexpression. *Circ Res.* 94, 514-524.
- Toussaint O, Medrano EE, von Zglinicki T (2000). Cellular and molecular mechanisms of stress-induced premature senescence (SIPS) of human diploid fibroblasts and melanocytes. *Exp Gerontol.* 35, 927-945.
- Trinei M, Giorgio M, Cicalese A, Barozzi S, Ventura A, Migliaccio E, Milia E, Padura IM, Raker VA, Maccarana M, Petronilli V, Minucci S, Bernardi P, Lanfranccone L, Pelicci PG (2002). A p53-p66<sup>Shc</sup> signalling pathway controls intracellular redox status, levels of oxidation-damaged DNA and oxidative stress-induced apoptosis. *Oncogene.* 21, 3872-3878.
- Urbanek K, Torella D, Sheikh F, De Angelis A, Nurzynska D, Silvestri F, Beltrami CA, Bussani R, Beltrami AP, Quaini F, Bolli R, Leri A, Kajstura J, Anversa P (2005). Myocardial regeneration by activation of multipotent cardiac stem cells in ischemic heart failure. *Proc Natl Acad Sci U S A.* 102, 8692-8697.
- Wada T, Joza N, Cheng HY, Sasaki T, Kozieradzki I, Bachmaier K, Katada T, Schreiber M, Wagner EF, Nishina H, Penninger JM (2004). MKK7 couples stress signalling to G2/M cell-cycle progression and cellular senescence. *Nat Cell Biol.* 6, 215-226.
- Wiemann SU, Satyanarayana A, Tsahuridu M, Tillmann HL, Zender L, Klempnauer J, Flemming P, Franco S, Blasco MA, Manns MP, Rudolph KL (2002). Hepatocyte telomere shortening and senescence are general markers of human liver cirrhosis. *FASEB J.* 16, 935-942.
- Wlaschek M, Hommel C, Wenk J, Brenneisen P, Ma W, Herrmann G, Scharffetter-Kochanek K (2000). Isolation and identification of psoralen

plus ultraviolet A (PUVA)-induced genes in human dermal fibroblasts by polymerase chain reaction-based subtractive hybridization. *J Invest Dermatol.* 115, 909-913.

Zhou S, Palmeira CM, Wallace KB (2001). Doxorubicin-induced persistent oxidative stress to cardiac myocytes. *Toxicol Lett.* 121, 151-157.

## Figure legends

**Figure 1.** Response of neonatal rat cardiomyocytes to doxorubicin (DOX). Cells were incubated with a low ( $10^{-7}$  mol/L) or high ( $10^{-6}$  mol/L) concentration of DOX for 24 hours. **A**, Phase-contrast images showing morphologic changes. **B**, DNA fragmentation on agarose gels was visualized under UV light. **C**, Expression of caspase-3 (Casp-3) and the cleaved enzyme (Cl. Casp-3) was determined by immunoblotting with specific antibodies. **D**, Both high and low concentrations of DOX induced oxidative stress as determined by DCFH-DA fluorescence. After culturing for 24 hours, cardiomyocytes were treated with a high ( $10^{-6}$  mol/L) or low ( $10^{-7}$  mol/L) concentrations of DOX, diluent without DOX (control), or  $H_2O_2$  ( $10^{-5}$  mol/L) as a positive control. After a 1 hour incubation, fluorescence intensity was analyzed. Representative results are shown.

**Figure 2.** Increased numbers of SA  $\beta$ -gal-positive cardiomyocytes in aging and treated cells. **A**, Cardiomyocytes were incubated with  $10^{-7}$  mol/L DOX,  $10^{-5}$  mol/L  $H_2O_2$ , or diluent without oxidants (control) for 7 days. Cells were then stained for the presence of SA  $\beta$ -gal as described in the Materials and Methods. **B**, The percentage of SA  $\beta$ -gal-positive cells was calculated. Data are mean  $\pm$  SD ( $n=3$ ;  $p<0.05$  vs. control). blue: SA  $\beta$ -gal, brown:  $\alpha$ -sarcomeric actin. **C**, Representative images of a 2-month-old young rat heart showing very little staining for SA  $\beta$ -gal, a 11-month-old middle aged rat, a 24-month-old aged rat and a 2-month-old DOX-treated rat heart showing positive staining for SA  $\beta$ -gal. **D**, The percentage of SA  $\beta$ -gal-positive cells was calculated. Data are mean  $\pm$  SD ( $n=3$ ; \*,  $p<0.05$  vs. control, #;  $p<0.05$  vs. 11 months, #;  $p<0.05$  vs. 24 months).

**Figure 3.** Activation of cTnI assessed by immunoblotting with anti-phospho-cTnI antibody and anti-cTnI antibody. **A**, Phosphorylation of cTnI in cardiomyocytes from aged and young rats. Extracts of kidney from each sample were used as negative controls. **B**, Baseline phosphorylation of cTnI in DOX-treated neonatal cardiomyocytes. **C**, Time course of isoproterenol (ISP)-induced cTnI phosphorylation in untreated (a) and DOX-treated (b) cardiomyocytes. After stimulation with ISP ( $10^{-6}$  mol/L) for the indicated times, cells were washed in ice-cold PBS and cell lysates were prepared. Representatives of 3 independent experiments are shown (left side). Densitometric analysis of phospho-cTnI was performed. Data are mean  $\pm$  SD ( $n=3$ ;  $p<0.05$ , right side).


**Figure 4.** Representative Northern blots showing changes in mRNA levels. Total cellular RNA from cardiomyocytes was examined by Northern blot analysis. Genes are indicated of the left of the autoradiograms. Probes were radioactively labeled, differentially expressed cDNA fragments. RNA loading was normalized to that of 18S rRNA.

**Figure 5.** Telomerase activity. **A**, Right panel; Representative telomeric repeat amplification protocol assay gel with samples of cultured neonatal rat cardiomyocytes (control and DOX-treated) and aged cardiomyocytes, which shows the characteristic telomerase-specific ladder and the 36-bp internal standard. Samples treated with heat inactivation were used as negative controls and Hela cells were used as positive controls. Left panel; The intensity of the ladders formed by TRAP assay was quantitated by Image J software and expressed as height using an internal standard. Data are mean  $\pm$  SD ( $n=3$ ; \*,  $p < 0.05$  vs. DOX-treated neonatal cardiomyocytes at day 1, #;  $p < 0.05$  vs. cardiomyocytes of 2 month-old rat). **B**, Expression of telomerase reverse transcriptase (TERT) was determined by immunoblotting with specific antibodies. **C**, Telomeric shortening in both DOX-treated and aged cardiomyocytes evaluated by Q-FISH. Labeling of telomeres in cardiomyocyte nuclei of adult young (2 months old)(1), aged (24 months old)(2), cultured neonatal non-treated (3) and a DOX-treated cultured neonatal (4) rat cardiomyocytes. Individual telomeres in nuclei (DAPI: blue fluorescence) are identified by green fluorescence (magnification bar: 10 $\mu$ m). Intensity of green fluorescence in cardiomyocyte nuclei from the aged and DOX-treated rat heart (2,4) was lower than that in the young and non-treated heart (1,3). The graphs on the right show the distribution of the fluorescence intensity of telomere spots in cardiomyocytes nuclei of each group. Cardiomyocytes show reduced mean (dashed line) and maximum values; a higher percentage of cells have minimum fluorescence intensity values (left shift).

**Figure 6.** Alterations in cell cycle regulatory protein expression. **A**, Expression of p21<sup>cip1/waf1</sup> and p27<sup>kip1</sup> were determined by immunoblotting with specific antibodies. **B**, Expression of p16<sup>INK4a</sup> was determined by RT-PCR. **C**, Expression of PML, p53 and acetyl-p53, shc, and phospho-shc<sup>p66</sup> were determined by immunoblotting with specific antibodies. **D**, Complex formation of PML with p53 or acetyl-p53 was determined by immunoprecipitation and immunoblotting with specific antibodies. Data are mean  $\pm$  SD ( $n=3$ ; \*,  $p<0.05$  vs. control).

**Figure 7.** p53 acetylation and protein expression in for DOX-treated cardiomyocytes were confirmed with the use of pifithrin- $\alpha$  (p53 expression inhibitor) or resveratrol (p53 acetylation inhibitor). **A**, Expression of p53, acetyl-p53 and p21<sup>cip1/waf1</sup> were determined by immunoblotting with specific antibodies. **B**, The percentage of SA  $\beta$ -gal-positive cells was calculated. Data are mean  $\pm$  SD ( $n=3$ ; \*,  $p<0.05$  vs. control, #;  $p<0.05$  vs. DOX). **C**, The effect of ISP-induced cTnI phosphorylation with the use of pifithrin- $\alpha$  or resveratrol in DOX-treated cardiomyocyte. **D**, The effect of telomerase activity in DOX-treated cardiomyocyte with the use of pifithrin- $\alpha$  or resveratrol. The intensity of the ladders formed by TRAP assay was quantitated. Data are mean  $\pm$  SD ( $n=3$ ; \*,  $p<0.05$  vs. control, #;  $p<0.05$  vs. DOX).

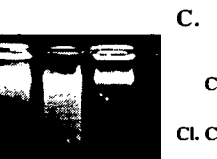
**A.**



Control       $10^{-6}$  mol/L       $10^{-7}$  mol/L

DOX

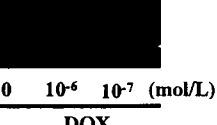
**B.**



0       $10^{-6}$        $10^{-7}$  (mol/L)

DOX

**C.**



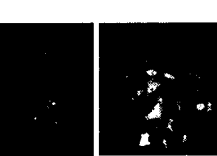
Casp-3

Cl. Casp-3

0       $10^{-6}$        $10^{-7}$  (mol/L)

DOX

**D.**



Control       $10^{-6}$  mol/L       $10^{-7}$  mol/L       $10^{-5}$  mol/L

DOX       $H_2O_2$

**A.**

Control

DOX ( $10^{-4}$  mol/L)

$H_2O_2$  ( $10^{-4}$  mol/L)

Cardiomyocyte

Non-myocyte

**B.**

(%)

SA  $\beta$  gal-positive cells

Control DOX  $H_2O_2$

$P < 0.05$

$P < 0.05$

N.S.

**C.**

2 months

11 months

24 months

DOX-treated

[400 $\times$ ]

**D.**

(%)

SA  $\beta$  gal-positive cells

2 months

11 months

24 months

DOX-treated

\*

\*\*#

\*\*†

**A.**

p-Troponin I

Troponin I

$\beta$ -actin

2 24 2 24 (months)

Heart Kidney

Density of p-Troponin I (fold)

2 24 (months)

Heart Kidney

**B.**

p-Troponin I

Troponin I

$\beta$ -actin

0 1 2 7 (days)

DOX ( $10^{-7}$  mol/L)

Density of p-Troponin I (fold)

0 1 2 7 (days)

DOX ( $10^{-7}$  mol/L)

**C.**

(a)

Isoproterenol ( $10^{-4}$  mol/L)

p-Troponin I

Troponin I

$\beta$ -actin

0 0.5 2 5 10 (minutes)

Control

Density of p-Troponin I (fold)

0 0.5 2 5 10 (minutes)

Control (minutes)

(b)

Isoproterenol ( $10^{-4}$  mol/L)

p-Troponin I

Troponin I

$\beta$ -actin

0 0.5 2 5 10 (minutes)

DOX ( $10^{-7}$  mol/L)

Density of p-Troponin I (fold)

0 0.5 2 5 10 (minutes)

DOX ( $10^{-7}$  mol/L) (minutes)

**Downregulated**

- SERCA2
- $\alpha$ -MHC
- GATA4
- Nkx2.5

**Upregulated**

- ANP
- Ang-II R
- 18SrRNA

0 1 2 7 (days) 2 24 (months)  
DOX ( $10^{-7}$  mol/L)

Figure 5

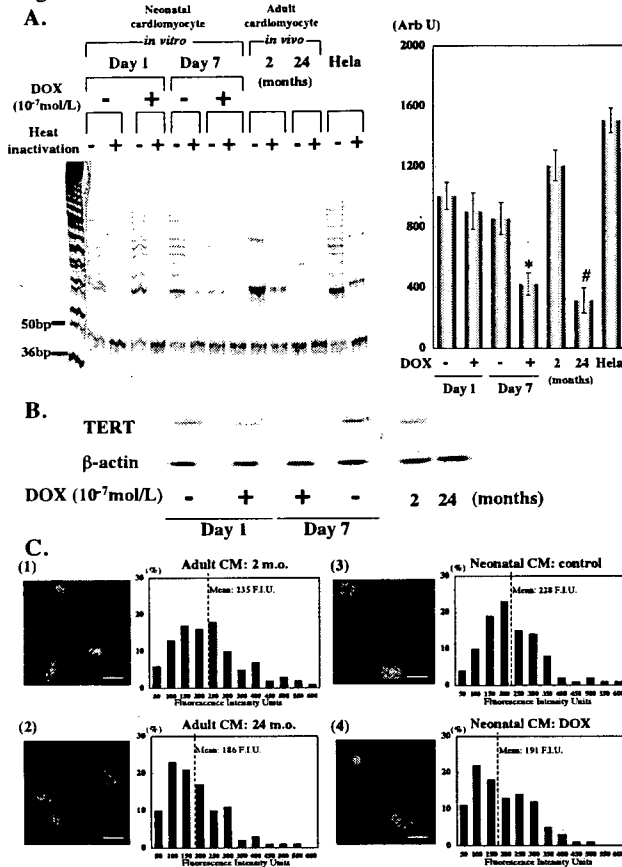


Figure 6

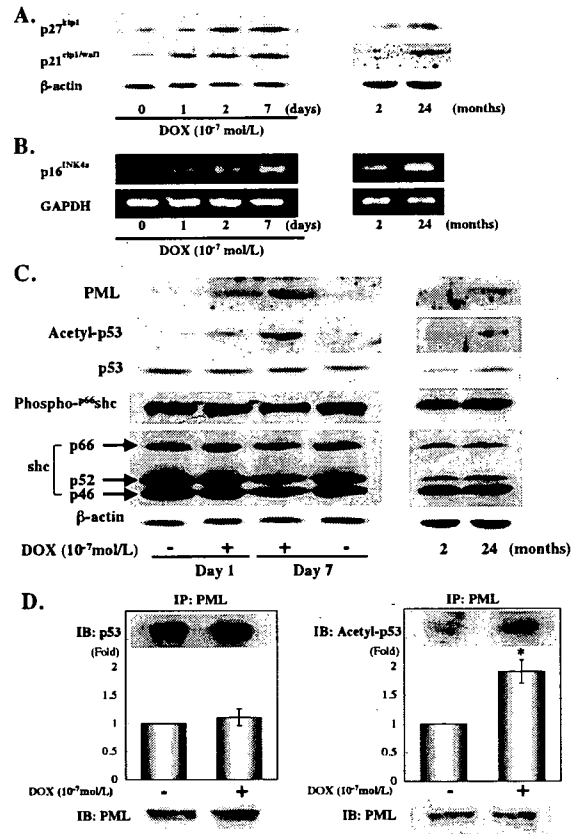
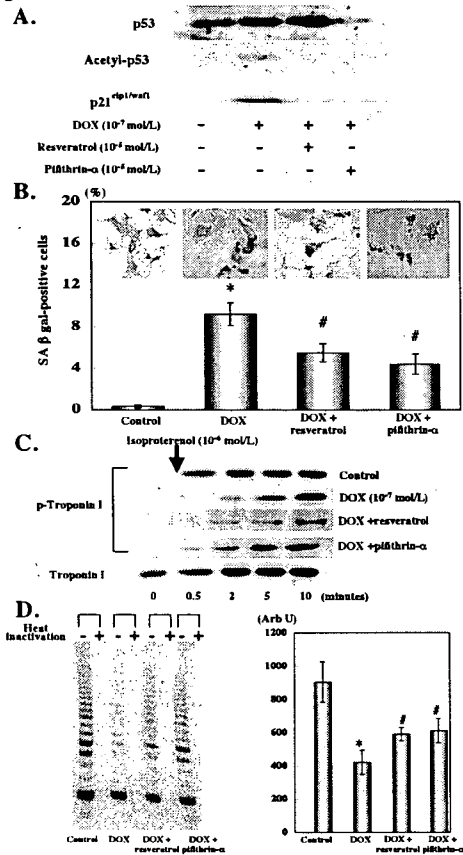


Figure 7



## Feasibility and safety of granulocyte colony-stimulating factor treatment in patients with acute myocardial infarction

Hiroyuki Takano<sup>a</sup>, Hiroshi Hasegawa<sup>a</sup>, Yoichi Kuwabara<sup>a</sup>, Takashi Nakayama<sup>a</sup>,  
Koki Matsuno<sup>b</sup>, Yoshiya Miyazaki<sup>b</sup>, Masashi Yamamoto<sup>c</sup>, Yoshihide Fujimoto<sup>c</sup>,  
Hisayuki Okada<sup>d</sup>, Shinji Okubo<sup>e</sup>, Miwa Fujita<sup>a</sup>, Satoshi Shindo<sup>a</sup>, Yoshio Kobayashi<sup>a</sup>,  
Nobuyuki Komiyama<sup>a</sup>, Noboru Takekoshi<sup>e</sup>, Kamon Imai<sup>d</sup>,  
Toshiharu Himi<sup>c</sup>, Iwao Ishibashi<sup>b</sup>, Issei Komuro<sup>a,\*</sup>

<sup>a</sup> Department of Cardiovascular Science and Medicine, Chiba University Graduate School of Medicine,  
1–8–1 Inohana, Chuo-ku, Chiba 260–8670, Japan

<sup>b</sup> Division of Cardiology, Chiba Emergency Medical Center, Chiba, Japan

<sup>c</sup> Department of Cardiology, Kimitsu Chuo Hospital, Kisarazu, Japan

<sup>d</sup> Division of Cardiology, Saitama Cardiovascular and Respiratory Center, Kohnan, Japan

<sup>e</sup> Division of Cardiology, Kanazawa Medical University, Uchinada, Japan

Received 21 July 2006; received in revised form 23 October 2006; accepted 2 November 2006

Available online 19 December 2006

### Abstract

**Background:** This study examined feasibility and safety of granulocyte colony-stimulating factor (G-CSF) treatment for patients with acute myocardial infarction (AMI).

**Methods:** Forty patients with AMI related with the left anterior descending coronary artery, who underwent successful percutaneous coronary intervention (PCI), were randomized into G-CSF group ( $n=18$ ) or Control group ( $n=22$ ). G-CSF treatment was started within 24 h after PCI.

<sup>99m</sup>Tc-tetrofosmin single-photon emission computed tomography (SPECT) was performed at 4 days and 6 months after AMI. SPECT data was analyzed for LV end-diastolic volume (LVEDV), LV end-systolic volume (LVESV), LV ejection fraction (LVEF) and myocardial perfusion.

**Results:** LVEF at 6 months was significantly better than that at 4 days in G-CSF group ( $p=0.013$ ), but not changed in Control group ( $p=0.245$ ). Although no significant difference was observed for LVEDV between the two groups, LVESV tended to be decreased only in G-CSF group. In G-CSF group, defect score (DS) was significantly decreased from 4 days to 6 months after AMI. Restenosis rate at 6 months after AMI was not significantly different between the two groups.

**Conclusions:** G-CSF treatment for patients with AMI was effective and did not have any clinical and angiographic adverse effects.

© 2006 Elsevier Ireland Ltd. All rights reserved.

**Keywords:** G-CSF; Myocardial infarction; Remodeling; Myocardial perfusion; Restenosis

### 1. Introduction

Therapeutic advances, in particular reperfusion therapies such as thrombolysis or percutaneous coronary intervention (PCI), have improved survival of patients with acute myocardial infarction (AMI). However, the number of

patients suffering from heart failure after AMI is increasing [1,2]. It has been reported that injection of CD34<sup>+</sup> cells including bone marrow stem cells (BMSCs) induces neovascularization in the ischemic myocardium and improves cardiac function after AMI in rats [3]. The injection of both G-CSF and stem cell factor also improved cardiac function and reduced mortality after AMI in mice [4]. Several groups including ours reported that G-CSF has beneficial effects on cardiac remodeling and dysfunction

\* Corresponding author. Tel.: +81 43 226 2097; fax: +81 43 226 2557.

E-mail address: komuro-ky@umin.ac.jp (I. Komuro).

after AMI in various animal models [5–8]. It has been reported that G-CSF accelerates healing process and myocardial regeneration and that G-CSF attenuates early ventricular expansion after AMI through accumulation of collagen in the infarcted area [6,9]. Moreover, it was demonstrated that mesenchymal stem cells in bone marrow are mobilized into the infarcted area and differentiated into cardiomyocytes by G-CSF after MI in mice [10].

We have recently reported that G-CSF receptor is expressed in cardiomyocytes and that G-CSF induces the activation of signaling molecules including Jak/STAT in cardiomyocytes [8]. Pretreatment with G-CSF significantly reduced the number of hydrogen peroxide-induced apoptosis of cardiomyocytes. Hydrogen peroxide-induced downregulation of antiapoptotic proteins such as Bcl-2 and Bcl-xL, which are target molecules of the Jak–STAT pathway, was recovered by G-CSF [8]. The cardioprotective effects of G-CSF on post-AMI hearts were abolished in the transgenic mice which overexpressed dominant-negative STAT3 in cardiomyocytes [8]. These results suggest that G-CSF not only mobilizes stem cells or progenitor cells into injured myocardium but also has direct protective effects on cardiomyocytes.

In clinical studies, however, efficacy of G-CSF administration in patients with AMI is controversial. Moreover, it has been reported that G-CSF therapy led to the unexpected high restenosis rate in stented vessels and the increase in plaque destabilization [11,12]. To evaluate feasibility and safety of G-CSF treatment in patients with AMI, we performed a randomized controlled trial in patients with AMI after successful PCI.

## 2. Methods

### 2.1. Participants

Our study was initiated in March 2003. By February of 2005, we had prospectively enrolled 40 patients with acute ST-segment elevation MI. Patients were eligible if they were admitted within 12 h after onset of AMI with total occlusion of LAD alone and underwent successful PCI with bare metal stent implantation. Patients, who achieved successful reperfusion with Thrombolysis in Myocardial Infarction (TIMI) flow grade 3 reperfusion and showed stable vital signs for at least 12 h, were randomized into one of the two groups; Control or G-CSF group. Exclusion criteria were previous MI; angiographically significant lesions in right coronary artery and/or left circumflex coronary artery; persistent severe heart failure (greater than Killip class II); uncontrolled myocardial ischemia or ventricular tachycardia; culprit lesion of infarct related artery not feasible for PCI; age older than 80 years; malignant disease; serious current infection or hematological disorder.

### 2.2. Study protocol

The study was a prospective, randomized, single-blind, placebo-controlled multi-center trial within the following

hospitals: Chiba University Hospital, Kimitsu Chuo Hospital, Chiba Emergency Medical Center, Saitama Cardiovascular and Respiratory Center, and Kanazawa Medical University Hospital. The institutional review board of each hospital approved the study protocol. We obtained informed consent from patients after explaining the procedure and risk. Randomization was done by using minimization method, in which the previously defined confounding factors; age, gender, peak creatine kinase (CK) level and time between the onset and PCI, would be equally distributed between the groups. Randomization was done by a blinded independent coordinator; after randomization, study processes were not blinded. In the G-CSF group, patients were subcutaneously injected with G-CSF (Kirin Brewery Co., Ltd., Japan) at 2.5 µg/kg body weight/day for 5 days after PCI. In the Control group, the patients were subcutaneously injected with saline. A criterion for G-CSF discontinuation was a white blood cells (WBC) count reaching the threshold of 4000/mm<sup>3</sup>. All patients were intravenously administered heparin (10,000–15,000 U/day) according to the standard protocol. We assessed the safety of G-CSF therapy on the basis of: development of major adverse cardiac events (MACE) (death, new myocardial infarction, revascularization, admittance to hospital due to aggravation of ischemia or heart failure); clinical status including G-CSF-related bone pain, dyspnea and chest pain; biochemical tests including CK and C-reactive protein (CRP); electrocardiogram (ECG). The primary endpoint was changes in LV function and volume, which was measured by ECG-gated <sup>99m</sup>Tc-tetrofosmin myocardial single-photon emission computed tomography (SPECT). The secondary endpoint was a change in myocardial perfusion that was assessed with stress and rest SPECT images and the development of MACE.

### 2.3. Procedures

We performed ECG-gated dipyridamole stress <sup>99m</sup>Tc-tetrofosmin SPECT 4 days after PCI as baseline and at 6 months follow-up. <sup>99m</sup>Tc-tetrofosmin (185 MBq) was administered 3 min after infusion of 0.56 mg/kg of dipyridamole, and SPECT image acquisition was performed 60 min after injection of <sup>99m</sup>Tc-tetrofosmin. Four hours later, ECG-gated SPECT image was acquired after administration of <sup>99m</sup>Tc-tetrofosmin (555 MBq) at rest. In ECG gating, SPECT data divided into 16 equal intervals were analyzed for LV end-diastolic volume (LVEDV), LV end-systolic volume (LVESV) and LV ejection fraction (LVEF) by quantitative gated SPECT (QGS) analysis. Gated tetrofosmin projection images were reconstructed and ventricular volumes and ejection fraction were calculated with Cedars quantitative gated single-photon emission CT software. The non-gated SPECT image was divided into 20 segments and each segment was graded with 4 scores between 0 and 3 (0 = normal uptake; 1 = mildly reduced uptake; 2 = moderately reduced uptake; 3 = defective) to assess the severity of myocardial perfusion abnormalities. The defect scores were



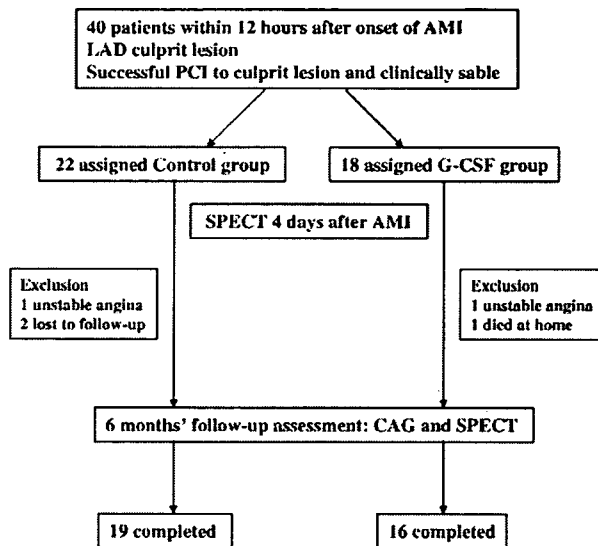


Fig. 1. Trial profile. LAD=left anterior descending coronary artery, PCI=percutaneous coronary intervention, SPECT=single-photon emission computed tomography, CAG=coronary angiography.

defined as the summation of the scores for LAD-related portion of LV in both the rest and stress images (DSL-rest and DSL-stress). SPECT data analysis was performed in a blinded fashion by two independent observers with no knowledge of the clinical status and medical therapy of patients.

Quantitative coronary angiography (QCA) was performed at baseline, immediately after PCI and at 6 months follow-up by an independent specialist with Encompass Review Station software (Heartlab Inc., Westerly, Rhode Island, USA). Minimal lumen diameter (MLD) and reference vessel diameter were measured from diastolic frames in single, matched views showing the smallest lumen diameter. Binary restenosis was defined as a diameter stenosis >50% within the stent or in the 5 mm segments proximal or distal to the stent at follow-up. To further examine the effect of G-CSF on atherosclerotic lesion, qualifying lesions were defined by  $25\% < \text{diameter stenosis} < 75\%$  in each of 10 proximal segments (segments 1, 2, 3, 5, 6, 7, 9, 11, 12, 13) at the baseline angiogram. All patients underwent follow-up visits every month after enrolment and were assessed for clinical status, safety, adverse reactions, and medication. If the culprit lesion was complicated with restenosis at follow-up coronary angiography, elective PCI was done at the investigators' decision.

Primary endpoint was the changes between global LVEF, LVESV and LVEDV at baseline and those after 6 months follow-up. Secondary endpoints were a change in defect scores and the difference in the incidence of MACE.

#### 2.4. Statistical analysis

Homogeneity of treatment groups at baseline was assessed using Student's *t* test for continuous variables and

Table 1  
Baseline characteristics of patients

	Control (n=22)	G-CSF (n=18)	p
Age (years)	63±11	61±8	0.908
Female/male	4/18	4/14	0.751
Max CK (IU/L)	3726±1734	3883±2515	0.817
Time to PCI (h)	4.9±2.6	6.5±5.6	0.225
Past history			
Hypertension	40.9%	44.4%	0.822
Diabetes mellitus	31.8%	33.3%	0.919
Hyperlipidemia	40.5%	33.3%	0.436
Current smoker	36.8%	50.0%	0.412
Medical treatment after admission			
Aspirin	100%	94.4%	0.263
Ticlopidine	95.5%	100%	0.360
Statins	54.6%	72.2%	0.251
Beta-blockers	40.9%	50.0%	0.565
ACE inhibitors or angiotensin receptor blockers	86.4%	94.4%	0.397

ACE = angiotensin-converting enzyme, CK = creatine kinase, PCI = percutaneous coronary intervention.

Chi-square test for categorical data. Changes in endpoints data between baseline and 6 months after G-CSF treatment were tested by paired Student's *t* test. Differences were considered significant if the *p*-value were <0.05. All data were expressed as mean±SD. Statistical analysis was done with SPSS version 11.5 (SPSS Inc. Chicago IL).

### 3. Results

#### 3.1. Patient characteristics

Forty patients with AMI related with the LAD, who underwent successful PCI and showed stable vital signs, were randomized into G-CSF group (2.5 µg/kg/day for 5 consecutive days, n=18) or Control group (saline, n=22) (Fig. 1). Six-month follow-up was completed in 16 of G-CSF

Table 2  
Peripheral circulating cells and biomarkers

		Entry	1 day	3 days	5 days
WBCs	Control	10.3±3.0	11.1±2.7	8.1±1.8	7.1±1.7
(10 <sup>3</sup> /mm <sup>3</sup> )	G-CSF	11.3±3.0	13.8±7.6	25.9±6.7*	29.4±9.0*
Neutrophils	Control	8.2±2.9	8.6±2.2	5.3±1.5	4.1±1.4
(10 <sup>3</sup> /mm <sup>3</sup> )	G-CSF	8.2±3.7	10.8±6.5	22.9±5.8*	23.6±6.7*
Lymphocytes	Control	2.0±1.3	1.8±1.0	2.1±1.0	1.8±0.6
(10 <sup>3</sup> /mm <sup>3</sup> )	G-CSF	2.0±1.1	2.0±1.1	2.7±1.1	2.6±1.0*
Monocytes	Control	0.5±0.3	0.6±0.3	0.8±0.3	0.7±0.2
(10 <sup>3</sup> /mm <sup>3</sup> )	G-CSF	0.6±0.4	1.0±0.6	1.3±0.6*	1.4±0.7*
Hemoglobin	Control	14.5±1.8	13.8±1.1	13.0±1.4	13.1±1.4
(g/dL)	G-CSF	14.7±1.8	13.4±1.4	12.7±2.0	13.0±1.9
Platelets	Control	224±66	205±51	191±46	216±48
(10 <sup>3</sup> /mm <sup>3</sup> )	G-CSF	214±78	192±77	181±76	211±74
CD34 <sup>+</sup>	Control	ND	0.9±0.6	ND	1.6±1.3
cells (μL)	G-CSF	ND	1.0±0.4	ND	15.0±18.9*
CRP (mg/dL)	Control	0.3±0.3	2.0±2.7	6.1±3.7	3.4±2.0
	G-CSF	0.5±0.5	2.1±2.3	7.2±3.4	3.9±2.3

ND = not determined. \**p*<0.05.

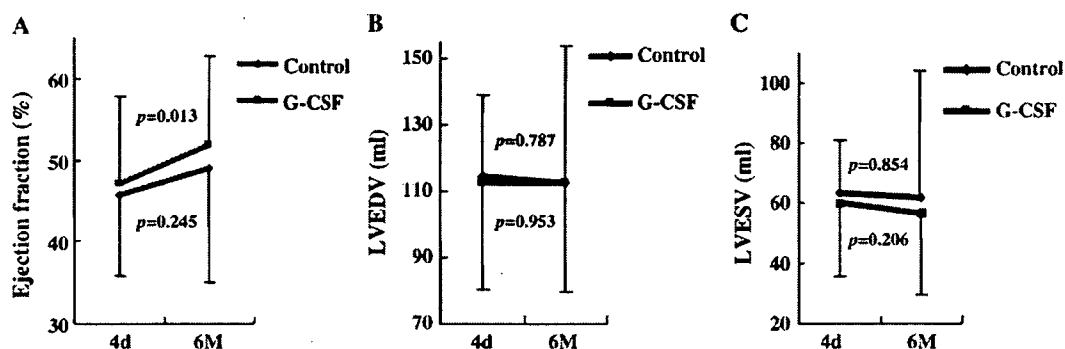


Fig. 2. Effects of G-CSF on LV function and volume after AMI. Changes in (A) LVEF, (B) LVEDV and (C) LVESV between baseline and 6 months in both groups. LVEDV=LV end-diastolic volume, LVESV=LV end-systolic volume.

group and 19 of Control group. The baseline characteristics of the studied population are shown in Table 1. The two groups were well matched for age, sex, past history and treatment after admission. There was no difference in max CK and time to PCI between the two groups. All patients were successfully subjected to primary PCI with stenting. G-CSF was well tolerated and the peak of peripheral WBC count was less than 40,000 in G-CSF group (Table 2). The patients in G-CSF group showed marked increases in the number of WBC, neutrophils, lymphocytes, monocytes and CD34<sup>+</sup> cells (Table 2). There were no changes in hemoglobin level and the number of platelets between 2 groups. Canadian Cardiovascular Society (CCS) score was 0 in all patients after PCI.

### 3.2. Effects of G-CSF on LV function and perfusion

We evaluated effects of G-CSF on LV function and myocardial perfusion by QGS analysis. LVEF evaluated by SPECT significantly improved after 6 months relative to baseline (4 days after AMI) in G-CSF group ( $47.2 \pm 10.6\%$  at 4 days;  $51.8 \pm 10.8\%$  at 6 months,  $p=0.013$ ) but not in Control group ( $45.6 \pm 9.7\%$  at 4 days;  $49.0 \pm 14.1\%$  at 6 months,  $p=0.245$ ) (Fig. 2A). There were no significant differences in LVEDV between baseline and 6 months in both G-CSF group ( $112.3 \pm 31.7\%$  at 4 days;  $112.6 \pm 32.9\%$  at 6 months,  $p=0.953$ ) and Control group ( $114.5 \pm 24.4\%$  at 4 days;  $112.5 \pm 40.9\%$  at 6 months,  $p=0.787$ ) (Fig. 2B). There was a trend of decrease in LVESV at 6 months compared with baseline in G-CSF group ( $60.3 \pm 24.4\%$  at 4 days;  $56.4 \pm 26.8\%$  at 6 months), although it was not significant ( $p=0.206$ ) (Fig. 2C). There was no decrease in LVESV at 6 months compared with baseline in Control group ( $63.2 \pm 17.6\%$  at 4 days;  $61.8 \pm 41.4\%$  at 6 months,  $p=0.854$ ) (Fig. 2C). Dipyridamole stress  $^{99m}\text{Tc}$ -tetrofosmin SPECT was performed at baseline (4 days after AMI) and 6 months follow-up for assessment of myocardial perfusion. In both groups, DSL-rest, which is indicative of the extent of MI, was significantly decreased after 6 months compared with baseline (Fig. 3A). DSL-stress, which indicates the extent of MI and ischemia, was also

significantly decreased in G-CSF group ( $12.8 \pm 7.3$  at 4 days;  $9.1 \pm 5.4$  at 6 months,  $p=0.007$ ) but not Control group ( $13.5 \pm 6.6$  at 4 days;  $11.5 \pm 6.7$  at 6 months,  $p=0.058$ ) after 6 months compared with baseline (Fig. 3B). These results suggest that G-CSF treatment can ameliorate LV function and myocardial perfusion for the patients with AMI.

### 3.3. Adverse events

One patient of either group presented unstable angina with restenosis of the culprit lesion (diameter stenosis 90%) and was successfully treated with cutting balloon. One patient in G-CSF group died at the next day after discharge (at 8 days after PCI). The patient was 63-year-old male with a history of smoking and hyperlipidemia. He was admitted to the hospital at 4 h after severe chest pain. Coronary angiography revealed total occlusion of LAD. The culprit lesion was successfully stented at 5 h after AMI. Max CK was 4360 IU/L. On telemetry monitoring, he was found to have many episodes of nonsustained ventricular tachycardia immediately after PCI. Since risky arrhythmia was not recognized during hospitalization, he was discharged at

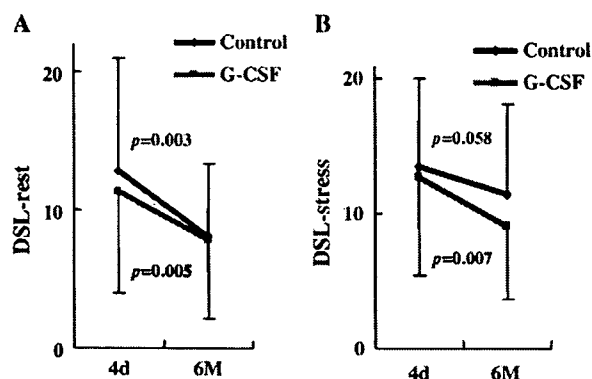


Fig. 3. Effects of G-CSF on myocardial perfusion after AMI. Changes in (A) DSL-rest and (B) DSL-stress between baseline and 6 months in both groups. DSL-rest=summation of defect scores for LAD-related portion of LV in rest image, DSL-stress=summation of defect scores for LAD-related portion of LV in stress image.

Table 3  
Quantitative coronary analysis

	Immediately after PCI	6 months	<i>p</i>
Control (28 lesions)			
MLD (mm)	2.34±0.670	2.42±0.78	0.656
Diameter stenosis (%)	38.0±9.9	36.8±10.9	0.691
Rate of restenosis at culprit lesion (%)		26.3	
G-CSF (21 lesions)			
MLD (mm)	2.11±0.50	2.11±0.51	0.995
Diameter stenosis (%)	39.5±10.7	39.2±12.0	0.854
Rate of restenosis at culprit lesion (%)		25.0	

MLD = minimal lumen diameter.

7 days after PCI. Autopsy was not performed and the cause of death was not known. All the completed patients were clinically stable and no major events such as heart failure, arrhythmia and thrombosis occurred during the follow-up period. To evaluate the rate of restenosis at culprit lesion, MLD and diameter stenosis, angiographic follow-up was performed at 6 months after AMI for all patients. There were no significant changes in MLD and diameter stenosis during 6 months in both 28 lesions in Control group and 21 lesions in G-CSF group (Table 3). We did not find the progression of atherosclerotic lesions in all coronary arteries except the culprit lesion of AMI in both groups. There was no significant difference in the rate of restenosis at culprit lesion between Control group and G-CSF group (Control group 26.3%, G-CSF group 25%) (Table 3). Three patients with G-CSF treatment presented transient mild fever. No patients developed other adverse events such as diabetic retinopathy and cancer during the course of this study.

#### 4. Discussion

Our randomized controlled clinical trial addresses feasibility and safety of G-CSF therapy in patients with AMI. We demonstrated that G-CSF treatment significantly improved LVEF and myocardial perfusion at 6 months after AMI. LVESV in G-CSF group was decreased although it was not significant. There was no difference in the rate of restenosis at 6 months follow-up between Control group and G-CSF group, and G-CSF treatment did not progress atherosclerotic lesions. These results suggest that G-CSF treatment for patients with AMI is effective and safe.

Our and other groups have recently reported that treatment with G-CSF after AMI has beneficial effects on LV function and remodeling in animal models [5–10]. Orlic et al. [4] demonstrated that G-CSF increased mobilization of BMSCs and promoted the regeneration of cardiac myocytes and vessels in the infarcted region. However, recent studies have indicated that adult hematopoietic stem cells do not transdifferentiate into cardiac myocytes in murine MI model [13,14]. We have demonstrated that G-CSF activates the signaling pathway of Jak–STAT through G-CSF receptor in cardiomyocytes and shows protective effects on cardiomyo-

cytes [8]. This randomized controlled study suggests that G-CSF has protective effects on human infarcted hearts.

Although recent experimental results suggest that G-CSF treatment has beneficial effects on post-MI hearts, there are some reports indicating that an increase in the number of neutrophils is correlated with myocardial injury after AMI and that G-CSF may increase the risk of thrombotic events [15,16]. Therefore, we carefully selected the patients with AMI who have no significant stenotic lesions except a culprit lesion of LAD and underwent successful PCI with stenting to perform the present trial safely. It is difficult to interpret the results of LV function, remodeling and myocardial perfusion in the case of multivessel disease or unsuccessful revascularization. LVEF was significantly increased after 6 months compared with baseline value in G-CSF group but not Control group, suggesting that G-CSF has the additional effects on conventional therapy for AMI. The number of CD34<sup>+</sup> cells was significantly increased at 5 days after starting G-CSF treatment, but no correlation between CD34<sup>+</sup> cells count and improvement of LVEF was recognized in G-CSF group (data not shown). The patient whose LVEF was improved by G-CSF treatment, did not necessarily show an increase in CD34<sup>+</sup> cells. Because we used low dose of G-CSF (2.5 µg/kg), the change of CD34<sup>+</sup> cells count was smaller than that reported by other clinical studies. Since we performed this trial with the strict inclusion criteria as described above, prominent progressions of LV remodeling and dysfunction were not recognized at 6 months after AMI even in Control group. There were no significant differences in LVEDV from baseline to 6 months in both Control group and G-CSF group. Although there were no significant differences in the changes of LVESV from baseline to 6 months in both groups, a trend of decrease in LVESV during 6 months was recognized only in G-CSF group.

Hill et al. [12] reported that G-CSF (10 µg/kg) treatment for 5 days induced serious adverse events in high-risk patients with severe coronary artery disease in non-randomized study. Since all 16 patients had CCS functional class 3 or 4 angina despite of prior attempts at revascularization, there is a possibility that they had many destabilized plaques in their coronary arteries. Valgimigli et al. [17] also examined the effects and safety of G-CSF (5 µg/kg for 4 days) in patients with AMI who were subjected to PCI with stenting in a randomized trial. QGS analysis showed that the relative increases in LVEF and LVEDV tend to be higher and lower, respectively, in G-CSF group (*n*=8) compared with Control group (*n*=8) at 6 months follow-up. Statistical difference was not recognized in 2 groups. One patient in Control group and no patients in G-CSF group presented binary restenosis at 6 months follow-up coronary angiography. Kuethe et al. [18] examined that treatment with G-CSF (10 µg/kg for 7 days) in patients with AMI who were treated with PCI in a prospective, non-randomized study. SPECT imaging demonstrated that G-CSF group (*n*=14) significantly improved the regional wall motion, wall perfusion and LVEF compared with Control group (*n*=9) at 3 months after AMI. No severe side effects

were observed in the G-CSF group. Ince et al. [19] analyzed the effects and safety of G-CSF (10 µg/kg for 6 days) in patients with AMI who were subjected to PCI with stenting in a randomized study (FIRSTLINE-AMI). Echocardiographic analysis demonstrated that G-CSF treatment significantly improved LVEF and wall motion score index at 4 months. LVED diameter showed no change in G-CSF group ( $n=25$ ), whereas LVED diameter progressively enlarged in Control group ( $n=25$ ). On the contrary, Zohnhofer et al. [20] quite recently assessed the effects of G-CSF treatment (10 µg/kg for 5 days) in a larger number of patients with AMI who has successful reperfusion by PCI in a randomized trial (REVIVAL-2). SPECT and magnetic resonance imaging (MRI) were performed at baseline and at 4 to 6 months after AMI. There were no significant differences in the changes of the infarct size and LVEF between G-CSF group ( $n=56$ ) and Control group ( $n=58$ ). Ripa et al. [21] also reported that G-CSF treatment (10 µg/kg for 6 days) was safe but did not lead to further improvement in LV function after AMI in a randomized trial (STEMMI). LVEF improved similarly in G-CSF group ( $n=37$ ) and Control group ( $n=33$ ) measured by both MRI and echocardiography from baseline to 6 months. The G-CSF treatment was started from about 90 min after PCI in FIRSTLINE-AMI, whereas it was started from 5 days after AMI in REVIVAL-2. In STEMMI, the G-CSF treatment was started from 1 to 2 days after AMI. Our patients were subjected to PCI at about 5–6 h after AMI and the G-CSF treatment was started from about 21 h after AMI. These findings suggest that the difference in time from AMI to PCI and/or G-CSF treatment contributes to the difference in outcome. We have recently reported that the beneficial effects of G-CSF were reduced when the G-CSF treatment was started late in MI mice model [8]. The timing of the treatment may be very critical to obtain the beneficial effects of G-CSF.

In the present study, one patient was dead at 8 days after AMI. The patient developed ventricular tachycardia immediately after PCI. Afterward, fatal arrhythmia was not recognized without anti-arrhythmic agents and he was discharged at 7 days after AMI. Since he was living alone, conditions including the existence of symptoms before death was unknown. It was also unknown whether his compliance for medication including anti-platelet drugs was good. Since subacute stent thrombosis occurs at a rate of 0.5–2% in elective cases and at 6% in patients with acute coronary syndromes despite anti-platelet therapy [22], it is unknown whether G-CSF treatment causes the event.

Another interesting result is that G-CSF did not increase the rate of restenosis at the culprit lesion. Kang et al. [11] found unexpectedly high rate of in-stent restenosis in patients with AMI or OMI, who were subjected to subcutaneous injections of G-CSF (10 µg/kg) for 4 days before PCI. Although the reason for the discrepancy is unknown at present, the study protocol (eg. dose and timing of G-CSF treatment) and patient population (eg. AMI or OMI, infarct-related coronary artery, number of patients) were different. In their study, patients did not receive primary PCI during the

golden time of AMI treatment and were treated with G-CSF for 4 days prior to PCI and only a few patients were assessed by coronary angiography at 6 months follow-up. We also found no progression of atherosclerotic lesions at 6 months follow-up in both groups. Our observations suggest that G-CSF can be used safely even in patients with atherosclerosis.

In contrast to the previous studies, we selected 40 AMI patients with total occlusion of LAD alone and underwent successful PCI with stent implantation in the present study to make evaluation of the results more accurate. We evaluated the effects of G-CSF on AMI patients in a prospective, randomized, single-blind, placebo-controlled multi-center trial. Furthermore, low dose of G-CSF (2.5 µg/kg) was used in our study to prevent a marked increase in WBC count and minimize adverse events by G-CSF. We determined the dose of G-CSF which does not increase WBC count over 40,000. Since inter-observer variability is often large in the analysis by echocardiography in the case of multi-center trial, we evaluated LV function and size by SPECT in the present study. SPECT is one of the most valuable modalities to evaluate the ischemic size and cardiac function. However, it is difficult for SPECT to correctly assess the ischemia when multiple coronary arteries have stenoses. To evaluate the effects of G-CSF on LV remodeling after AMI precisely by SPECT, it was necessary to select the patients of one vessel disease. Inclusion criteria of patients, the number of patients, protocols and the methods of assessment are also very important to evaluate feasibility and safety of novel therapies.

This study does have limitations. First, because we restricted the enrolled patients of total occlusion of LAD alone and underwent successful PCI with stent implantation in the present study, the number of patients may be too small to detect the significant difference in improvement in myocardial function and perfusion between two groups. Second, the study was single-blind, such that patients were not aware of whether they were receiving G-CSF or saline. However, the concealment of allocation and the use of an objective, blinded, endpoint assessment strengthened the significance of the results. Third, because G-CSF treatment was started within 21 h after AMI in our study, there is a possibility that the earlier start of the treatment would result in better effects. Further studies are needed to elucidate when the treatment should be started. Finally, we used low dose (2.5 µg/kg) of G-CSF to minimize possible adverse events such as an increase in circulating WBC count by G-CSF. The beneficial effects of G-CSF may be more if higher dose of G-CSF is used.

## 5. Conclusion

We demonstrated feasibility and safety of G-CSF treatment in randomized controlled trial. Our results suggest that the treatment with low dose of G-CSF is effective and safe in AMI. It remains to be determined how much dose of G-CSF is optimal and when the treatment should be started. Further studies are needed to establish the most effective and the less adverse regimen of G-CSF treatment.